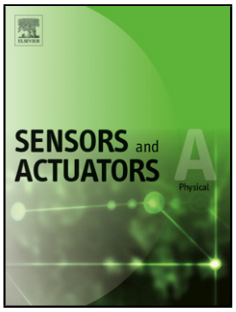

Title: A High Sensitivity Temperature Sensor Based on
Packaged Microfibre Knot Resonator

Authors: Jin Li, Liting Gai, Hanyang Li, Haifeng Hu

PII: S0924-4247(17)30250-9
DOI: http://dx.doi.org/doi:10.1016/j.sna.2017.06.031
Reference: SNA 10190

To appear in: *Sensors and Actuators A*

Received date: 9-2-2017
Revised date: 17-6-2017
Accepted date: 27-6-2017

Please cite this article as: Jin Li, Liting Gai, Hanyang Li, Haifeng Hu, A High Sensitivity Temperature Sensor Based on Packaged Microfibre Knot Resonator, Sensors and Actuators: A Physicalhttp://dx.doi.org/10.1016/j.sna.2017.06.031

A High Sensitivity Temperature Sensor Based on Packaged Microfibre Knot Resonator

Jin Li[1, 2, *], Liting Gai[1], Hanyang Li[3], and Haifeng Hu[1]

[1]*College of Information Science and Engineering, Northeastern University, Shenyang, 110819, China*

[2]*Laser Physics Centre, Australian National University, Canberra, Australian Capital Territory 2601, Australia*

[3]*Key Lab of In-fibre Integrated Optics, Ministry of Education of China, Harbin Engineering University, Harbin 150080, China*

*Corresponding author: lijin@ise.neu.edu.cn

All authors' telephone numbers and e-mail address:

Jin Li

Telephone number: +86-13610885247; Email: lijin@ise.neu.edu.cn

Liting Gai

Telephone number: +86-18842397493; Email: 1902596409@qq.com

Hanyang Li

Telephone number: +86-13613623072; Email: hanyang_li@qq.com

Haifeng Hu

Telephone number: +86-24-83687266; Email: huhaifeng@ise.neu.edu.cn

A High Sensitivity Temperature Sensor Based on Packaged Microfibre Knot Resonator

A novel temperature sensor has been proposed based on microfibre knot resonator packaged by polydimethylsiloxane (PDMS). Owing to the high thermal expansion and thermo-optic coefficients of PDMS, the resonant wavelength shifted obviously along with the changing of temperature. The experimental results indicated the approximate linear temperature sensing performance in the range of 24–38 ℃ and 40–54 ℃, with the high sensitivities of 1.408nm/ ℃ and 0.973 nm/℃, respectively. Due to its excellent performances and easy fabrication process, the temperature sensor will be the promising candidate for monitoring the stability of air condition and organism.

Highlights

- 1. A compact sensor chip based on MKR packaged by PDMS was proposed;
- 2. The temperature sensing characteristics has been experimentally demonstrated;
- 3. The detection sensitivity is experimentally demonstrated as 1.408nm/℃.

A High Sensitivity Temperature Sensor Based on Packaged Microfibre Knot Resonator

(

Abstract)

A novel temperature sensor has been proposed based on microfibre knot resonator packaged by polydimethylsiloxane (PDMS). Owing to the high thermal expansion and thermo-optic coefficients of PDMS, the resonant wavelength shifted obviously along with the changing of temperature. The experimental results indicated the approximate linear temperature sensing performance in the range of 24–38℃ and 40–54℃, with the high sensitivities of 1.408nm/℃ and 0.973nm/℃, respectively. Due to its excellent performances and easy fabrication process, the temperature sensor will be the promising candidate for monitoring the stability of air condition and organism.

Keywords: Fibre sensors; Optical sensing and sensors; Optical resonators.

Keywords: Fibre sensors; Optical sensing and sensors; Optical resonators.

1. Introduction

Some compact and robust sensors, including the optical microfibre/nanofibre (MNF) based sensors, have aroused a wide interest and proverbially studied due to their good selectivity, high sensitivity, non-intrusive features, and fast response time (*1*-*3*). The unique advantages of MNF resonant ring sensors, such as small size, anti-interference, quick response, high resolution, low detection limit and high sensitivity (*4*-*8*), have promoted their enormous potential applications in measuring refractive index (RI), temperature, bio-chemical analyte, current, displacement, force, electric field, and magnetic field (*9*-*12*). Light can transmit through the MNF in a form of evanescent wave to highly sense the variation of surrounding environment (*13*, *14*). In a typical MNF resonant ring, the light will be split into two parts. Where one part transmits along the ring fibre, then interferes with another part transmitted in the bus fibre. When the external parameters changes, both the effective RI and the length of the MNF ring change accordingly, resulting in the shift of resonant wavelength (*15*). The corresponding changes thus can be obtained. Among different kinds of MNF resonating rings, the micro-loop resonator (MLR), micro-knot (MKR) resonator and micro-coil resonator (MCR) have been mainly studied (*16*). Being the most simple and unstable structure, MLR can be fabricated by self-coupling method. MCR is usually combined with microfluidics technology to measure biological and chemical analyte. In comparison with MLR and MCR, MKR is an excellent MNF ring resonator due to its stable performances and adjustable free spectral range (FSR). Xu et al. (*17*) demonstrated a compact MKR temperature sensor with a sensitivity of 0.28 nm/℃. Yang et al. (*18*) designed a seawater temperature sensor based on a MKR and obtained a sensitivity of 22.81 pm/℃.

In this paper, we proposed a novel temperature sensor based on MKR packaged by polydimethylsiloxane (PDMS). A higher sensitivity, better stability and repeatability performance than those of the bare MKR were experimentally obtained. Compared with the temperature sensors based on other fibre structures, such as fibre coupler, fibre Bragg grating, Sagnac interferometer, Fabry-Perot interferometer, microfiber taper and high-order modes interferometer, this temperature sensor has the advantages of small size, simple manufacture, compact structure, low cost, easy to carry and convenient to integrate with other fibre systems.

2. Theoretical analysis

Firstly, the MNF ring splits the light into two parts and produces the resonance enhancement effect. One part of light resonates in the ring fibre and builds a harmonic electromagnetic field, while the other part transmits along the bus fibre directly and couples with the resonating light. The resonance frequency is determined by the condition: $2\pi Rn_{eff}=m\lambda_m$, n_{eff} is the effective index of microfiber and R is the radius of MKR. FSR is given as λ^2/n_gL (*19*), λ is the wavelength, n_g is the mode propagating index in the microfiber, and L is the loop length. When the external temperature changes, the loop length L and mode propagating index n_g vary accordingly, results in the peak shift of resonant wavelength. The relative variation can be expressed as $\Delta\lambda/\lambda = (\Delta L/L+\Delta n/n)_{temp} = [\alpha_s+1/n_s(dn_s/dT)+\alpha_p+1/n_p(dn_p/dT)]\Delta T$, α_s and α_p are the thermal expansion coefficients of microfiber and PDMS, respectively. Here, α_s can be ignored because α_s and α_p are $\sim 5.5\times10^{-7}$ and $\sim 3\times10^{-4}$, respectively; dn_s/dT and dn_p/dT are the thermo-optic coefficients of microfiber and PDMS, which are $\sim 1.1\times10^{-5}$ /℃ and $\sim -5\times10^{-4}$ /℃, respectively. The effect of the external refractive index and the length of resonant ring on transmission spectra was simulated by R-soft, where the diameter of microfiber maintained as 0.2 μm and the length of the resonant ring changed from 1.6 μm to 1.9 μm. As the length increasing, the bigger wavelength blue shift has been revealed with a factor of 55.25nm/μm. The big thermal expansion coefficient of PDMS (~3×10^{-4}) resulted a high temperature sensitivity. When the diameter of microfiber and the resonant ring were fixed as 0.2 μm and 1.6 μm, respectively, the wavelength blue shift was observed with the decrease of the external refractive index. This result was contributed to the big and negative thermo-optic coefficients of PDMS (~-5×10^{-4} /℃). From the theoretical results, it is concluded that the introduction of PDMS coating layer can significantly improve the sensitivity of MKR temperature sensor. For a thicker microfiber (0.4μm) with the same length (1.6μm), the refractive index sensitivity reduced from 81nm/RIU to 45nm/RIU. Therefore, the sensitivity of this MKR temperature sensor can be further improved by using a thinner microfiber in the future work.

3. Experiment setup

In experiment, a uniform microfiber with a diameter of 10.26 μm was fabricated from the standard single mode fibre (SMF) with a two-step stretching method reported earlier (*20*). The prepared microfiber was cut into two sections with free ends and fixed on the 3D fibre adjustments. A tungsten probe was used to knot the free end of microfiber into a ring structure under microscope. The micrograph of knot region is shown in Fig.1 (a).

By micro-pulling the free end of knot structure, the diameter and corresponding FSR could be manipulated easily. The MKR structure is stable due to the Vander Waals force and static electricity between MNFs. In experiment, a MKR with the diameter of 4.5 mm was prepared. Both the SMF tapers and the MKR were placed on an MgF_2 substrate (RI ~1.37, results in a low optical loss) and micro-manipulated by 3D fibre adjustment (precision: 0.1 μm). PDMS is a kind of high transparent elastomer with low toxicity. The PDMS solution was prepared by mixing the basal component and the hardener component with a ratio of 10:1. The mixture has been standing quietly for two hours to eliminate air bubbles. The MKR structure immersed by PDMS solution has been cured at 80 ℃ for three hours. A thin layer of PDMS (~30 μm) was finally coated. Both ends of MKR were immobilized with UV glue to further enhance the stability. The light signal emitted by the amplified spontaneous emission (ASE) source was launched into a SMF taper (named input SMF taper), then coupled into MKR by the evanescent coupling method. The transmission optical signal was received by the optical spectrum analyzer (OSA) through another SMF taper (named output SMF taper). The schematic diagram was shown in Fig. 1. To characterize the optical confine performance, the 632.8 nm laser was launched into the MKR structure, as shown in Fig. 1 (b). The inset shows the enlarge micrograph of the ring section. In addition to the scattering on the edge of MgF_2 substrate, the light was confined inside the MNF and transmitted through effectively.

4. Experimental results and discussion

To explore the temperature sensing performance, a water bath kettle and a thermocouple were used to promise a constant temperature environment. When the temperature increased continuously from 24 ℃ to 38 ℃ by a step of 2 ℃, the sensing performance was determined by tracing the resonant dip in the transmission spectra, as shown in Fig. 2 (a). The resonant dip blue-shifted with the increase of the external temperature during the wavelength region less than one FSR. The sensitivity of 1.408 nm/℃ was obtained during heating process. When the external temperature decreased from 38 ℃ to 24 ℃ by a step of 2 ℃, the same resonant dip red-shifted with a sensitivity of 1.469 nm/℃. As shown in Fig. 2 (b), a slight hysteresis error was observed between heating and cooling process attributed to the restriction of some experimental conditions, such as the measuring exactness, instability distribution of temperature, and the uniformity or smoothness of MNF.

To verify the stability and repeatability, other twice experiments were carried out under the same conditions. The resonance wavelength was recorded during heating process from 24 °C to 38 °C by a step of 2 °C. Three groups of experimental data and the corresponding linear fitting curves were illustrated in Fig. 3. The sensor shows a remarkable stability and the small difference in sensitivity caused by the random noise during experiment. In addition to the experiment result presented earlier in Fig. 2, the sensitivities of 1.413 nm/°C and 1.406 nm/°C were obtained for two other heating process from 24 °C to 38 °C, while the sensitivities of 1.458 nm/°C and 1.464 nm/°C were observed during cooling process from 38 °C to 24 °C. The experimental results indicated that this packaged MKR structure performed the high sensitivity of more than 1.4 nm/°C with a good linearity in the range of 24–38 °C. Due to the 20 pm resolution of OSA used in this work, the temperature sensing accuracy could be limited less than 0.014 °C, which was more excellent than some commercial temperature sensors. The temperature sensing limit can be enhanced further less than 0.008 °C by using the demodulator with a higher resolution (<10 pm). The outstanding sensing performance enables its promising application in monitoring the stability of air condition and organism. However, when the temperature increased continually from 40–54 °C, the sensitivity would be limited by the thermal expansion effect of PDMS, which also resulted a worse linearity. As shown in Fig. 4, the poorer sensitivities of 0.973 nm/°C and 0.956 nm/°C were experimentally revealed. It was found that this temperature sensor was more sensitive in 24→38 °C. Furthermore, the sensitivity maybe improved further by diminishing the diameter of MNF, reducing the ring diameter of MKR, and introducing some functional materials with excellent thermal expansion properties. Moreover, the packaging process could be optimized by coating another transition film on the PDMS to expand the working range. To explore the stability of the temperature sensor, we monitored the location of the resonance dip using spectrograph for five different constant temperature values, including 30.2 ℃, 35.35 ℃, 40.36 ℃, 44.23 ℃ and 47.2 ℃. Ten locations were continuously recorded with an interval of 5 minutes for each value, as indicated in Fig. 5, where the resonance wavelength was demonstrated with an excellent stability performance (floating range <0.01 nm).

5. Conclusion

In conclusion, a PDMS-packaged MKR structure has been prepared. The temperature sensitivity was demonstrated significantly to be up to 1.408 nm/℃ during the heating process of 24→38 ℃, and 1.469 nm/℃ in the cooling process of 38→24 ℃. Furthermore, the sensitivities of 0.973 nm/℃ and 0.956 nm/℃ were experimentally verified during the processes of 40→54 ℃ and 54→40 ℃, respectively. Due to its compact size, low cost and stable layout, the proposed MKR temperature sensor provides a potential way to fabricate the independent sensor probes or chips. And the sensing performances can be effectively improved by encapsulating with functional materials and adjusting morphology parameters.

Funding Information.

Biographies

Jin Li is Associated Professor in the department of Information Science and Engineering at Northeastern University, China since Dec. 2013. He was born in the city of Yuncheng, Shan Xi Province, China in Dec. 1983. He earned the bachelor degree in Electronic Science and Technology at Harbin Institute of Technology (HIT), China in 2007, Master's degree in Physical Electronics at HIT, China in 2009, Doctor's degree in Physical Electronics at HIT, China in 2013. His research interests include surface plasmon, nano-structured optics, nonlinear optics and fiber sensors.

Liting Gai was born in the city of Zhaodong, Heilongjiang Province, China, in Jan. 1993. She is currently pursuing a Master’s Degree in the Research Center of Optical Sensing and Detection Technology as a Master. Her research interest is microfiber sensor.

Hanyang Li is Lecturer in the Key Lab of In-fiber Integrated Optics, Ministry Education of China, Harbin Engineering University, China since 2015. He was born in the city of YiChun, Heilongjiang Province, China in Nov. 1982. He earned the bachelor degree in Inorganic Chemistry at Heilongjiang University, China in 2007, Master's degree in Inorganic Chemistry at HIT, China in 2009, Doctor's degree in Inorganic Chemistry at HIT, China in 2013. His research interests include fiber sensor, nonlinear optics, laser-matter interaction and micro/nano laser.

Haifeng Hu is Lecturer in the department of Information Science and Engineering at Northeastern University, China since Jun. 2013. He was born in the city of Liaoyang, Liao Ning Province, China in Dec. 1984. He earned the bachelor degree in Electronic Science and Technology at JiLin University, China in 2007, Doctor's degree in Microelectronics and Solid State Electronics at Institute of Semiconductors, Chinese Academy of Sciences, China in 2013. His research interests include surface plasmon photonics, SPR fiber based detection technology and bio-sensing technology.

This work was supported by the National Natural Science Foundation of China (NSFC) under Grants (number 61405032, 61403074, 61605031, 61425003); and Doctoral Scientific Research Startup Foundation of Liaoning Province under Grant (number 201501144); and Fundamental Research Funds for the Central Universities under Grants (number N150404022, N150401001). Jin Li acknowledges the financial support from the China Scholarship Council for his Visiting Scholarship No. 201606085023.

References

(1) Jiang, H. M.; Yang, R. D.; Tang, X. L.; Burnett, A.; Lan, X. W.; Xiao, H.; Dong, J. H. Multilayer fibre optic sensors for in situ gas monitoring in harsh environments. *Sensor. Actuat. B-Chem.* **2013,** *177,* 205–212.

(2) Qazi H. H., Mohammad A. B., Ahmad H., Zulkifli M. Z., Harun S. W. Single-mode D-shaped optical fibre sensor for the refractive index monitoring of liquid. *J. Mod. Optic.* **2016,** *63,* 750-755.

(3) Ji, W.B.; Liu, H.H.; Tjin, S. C.; Chow, K.K.; Lim, A. Ultrahigh sensitivity refractive index sensor based on optical microfibre. *IEEE Photon. Tech. Lett.* **2012,** *24,* 1872–1874.

(4) Lorenzi, R.; Jung, Y. M.; Brambilla, G. In-line absorption sensor based on coiled optical microfibre. *Appl. Phys. Lett.* **2011,** *98,* 173504.

(5) Ding, M.; Wang, P. F.; Brambilla, G. A microfibre coupler tip thermometer. *Opt. Express* **2012,** *20,* 5402-5408.

(6) Wu, Y.; Zhang, T. H.; Rao, Y. J. Miniature interferometric humidity sensors based on silica/polymer microfibre knot resonators. *Sensor Actuat. B-Chem.* **2011,** *155,* 258–263.

(7) Wu, X. Q.; Tong, L. M. Optical microfibres and nanofibres. *Nanophotonics* **2013,** *2,* 407–428.

(8) Jin, W.; Wang, C.; Xuan, H. F.; Jin, W. Tunable comb filters and refractive index sensors based on fibre loop mirror with inline high birefringence microfibre. *Opt. Lett.* **2013,** *38,* 4277–4280.

(9) Wang, P.; Gu, F. X.; Zhang, L.; Tong, L. M. Polymer microfibre rings for high-sensitivity optical humidity sensing. *Appl. Opt.* **2011,** *50,* G7–G10.

(10) Liu Q., Chen Y. PMMA-rod-assisted temperature sensor based on a two-turn thick-microfibre resonator. *J. Mod. Optic.* **2016,** *63,* 159-163.

(11) Lim, K. S.; Harun, S. W.; Damanhuri, S. S. A.; Jasim, A. A.; Tio, C. K.; Ahmad, H. Current sensor based on microfibre knot resonator. *Sensors and Actuat. A-Phys.* **2011,** *167,* 60–62.

(12) Li, X. L.; Ding, H. All-fibre magnetic-field sensor based on microfibre knot resonator and magnetic fluid. *Opt. Lett.* **2012,** *37,* 5187–5189.

(13) Wang, P. F.; Brambilla, G.; Ding, M.; Semenova, Y.; Wu, Q.; Farrell, G. High-sensitivity, evanescent field refractometric sensor based on a tapered, multimode fibre interference. *Opt. Lett.* **2011,** *36,* 2233–2235.

(14) Brambilla, G.; Finazzi, V.; Richardson, D. J. Ultra-low-loss optical fibre nanotapers. *Opt. Express* **2004,** *12,* 2258–2263.

(15) Guo, X.; Tong, L. M. Supported microfibre loops for optical sensing. *Opt. Express* **2008,** *16,* 14429–14434.

(16) Chen, G. Y.; Ding, M.; Newson, T. P.; Brambilla, G. A review of microfibre and nanofibre based optical sensors. *Open Opt. J.* **2013,** *7,* 32–57.

(17) Zeng, X.; Wu, Y.; Hou, C. L.; Bai, J.; Yang, G. G. A temperature sensor based on optical microfibre knot resonator. *Opt. Commun.* **2009,** *282,* 3817–3819.

(18) Yang, H. J.; Wang, S. S.; Wang, X.; Liao, Y. P.; Wang, J. Temperature sensing in seawater based on microfibre knot resonator. *Sensors-Basel* **2014,** *14,* 18515–18525.

(19) Xu, F.; Brambilla, G. Manufacture of 3-D microfibre coil resonators. *IEEE Photon. Technol. Lett.* **2007,** *19,* 1481–1483.

(20) Tong, L. M.; Gattass, R. R.; Ashcom, J. B.; He, S. L.; Lou, J. Y.; Shen, M. Y.; Maxwell, I.; Mazur, E. Subwavelength-diameter silica wires for low-loss optical wave guiding. *Nature* **2003,** *426,* 816–819.

Figure captions:

Figure 1. Schematic diagram of experimental setup for temperature measurement. (a) is the micrograph of knot region; (b) is the photograph of MKR lighted by 632.8nm laser on a MgF_2 substrate.

Figure 2. (a) Transmission spectra of fabricated MKR for temperature ranges from 24℃ to 38℃. (b) Single resonant wavelength changes as a function of temperature from 24℃ to 38℃ (black) and 38℃ to 24℃ (red), respectively. Dots and solid lines refer to experimental and numerical fitting results, respectively.

Figure 3. Three experimental sensing curves from 24℃ to 38℃ under same condition.

Figure 4. (a) Transmission spectra of fabricated MKR for temperature ranges from 40℃ to 54℃. (b) Single resonant wavelength changes as a function of temperature from 40℃ to 54℃ and 54℃ to 40℃, respectively. The black dots and the red dots represent the experimental data in 40℃ to 54℃ (black) and 54℃ to 40℃ (red), respectively. Dots and solid lines refer to experimental and numerical fitting results, respectively.

Figure 5. Temperature sensing stability for five different constant temperature values: 30.2 ℃, 35.35 ℃, 40.36 ℃, 44.23 ℃ and 47.2 ℃.

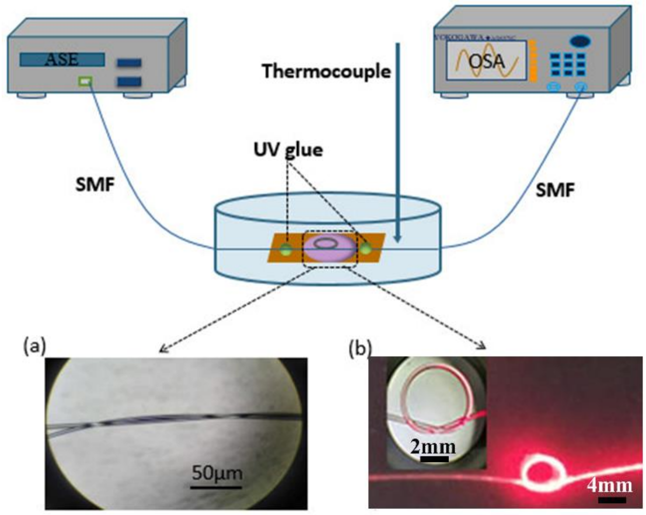

Figr-1

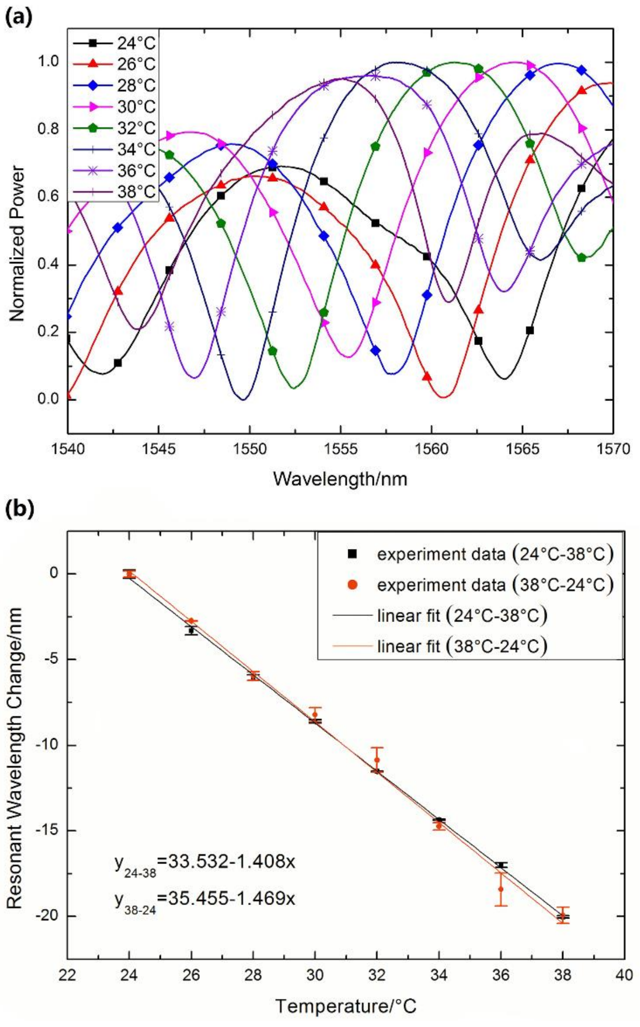
(a)
24°C
26°C
28°C
30°C
32°C
34°C
36°C
38°C
Normalized Power
0.0
0.2
0.4
0.6
0.8
1.0
1540
1545
1550
1555
1560
1565
1570
Wavelength/nm
(b)
experiment data (24°C-38°C)
experiment data (38°C-24°C)
linear fit (24°C-38°C)
linear fit (38°C-24°C)
Resonant Wavelength Change/nm
0
-5
-10
-15
-20
y24-38=33.532-1.408x
y38-24=35.455-1.469x
22
24
26
28
30
32
34
36
38
40
Temperature/°C

Figr-2

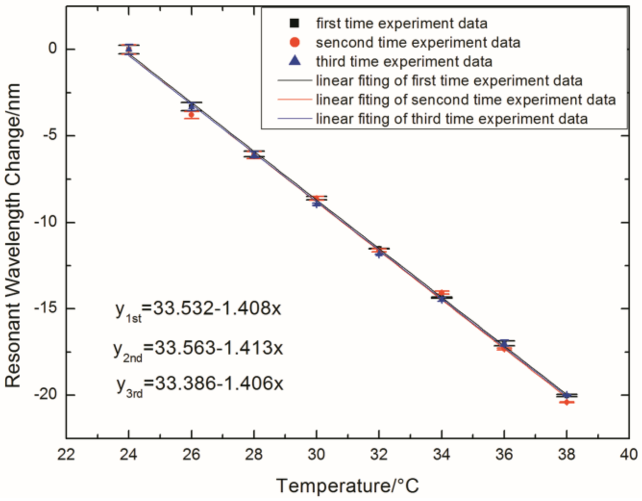
Resonant Wavelength Change/nm
Temperature/°C
0
-5
-10
-15
-20
22
24
26
28
30
32
34
36
38
40
■ first time experiment data
● sencond time experiment data
▲ third time experiment data
linear fiting of first time experiment data
linear fiting of sencond time experiment data
linear fiting of third time experiment data
y_{1st}=33.532-1.408x
y_{2nd}=33.563-1.413x
y_{3rd}=33.386-1.406x

Figr-3

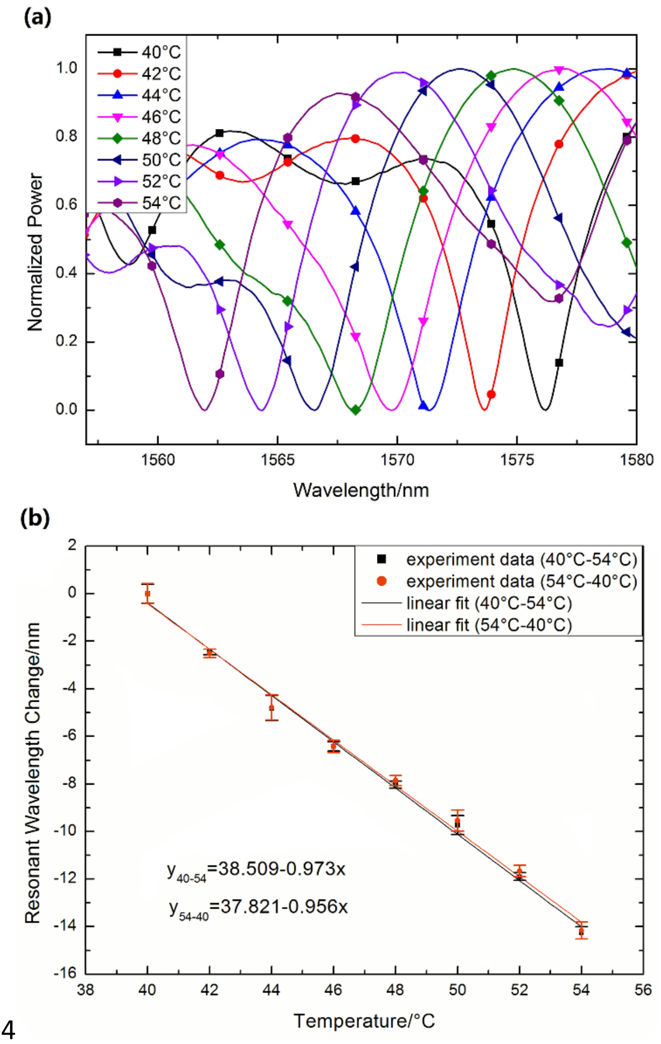
(a)
40°C
42°C
44°C
46°C
48°C
50°C
52°C
54°C
Normalized Power
0.0
0.2
0.4
0.6
0.8
1.0
1560
1565
1570
1575
1580
Wavelength/nm
(b)
experiment data (40°C-54°C)
experiment data (54°C-40°C)
linear fit (40°C-54°C)
linear fit (54°C-40°C)
Resonant Wavelength Change/nm
2
0
-2
-4
-6
-8
-10
-12
-14
-16
y40-54=38.509-0.973x
y54-40=37.821-0.956x
38
40
42
44
46
48
50
52
54
56
Temperature/°C

Figr-4

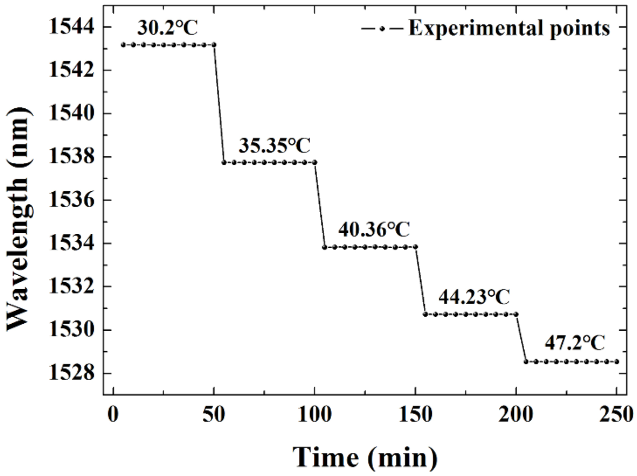
30.2℃
35.35℃
40.36℃
44.23℃
47.2℃
Experimental points
Wavelength (nm)
1528
1530
1532
1534
1536
1538
1540
1542
1544
Time (min)
0
50
100
150
200
250

Figr-5